

Jelena D. Gojčić<sup>1</sup>, Aleksandar M. Petričević<sup>1</sup>,  
Mila N. Krstajić Pajić<sup>1</sup>, Vladimir D. Jović<sup>2\*</sup>

<sup>1</sup>University of Belgrade, Faculty of Technology and Metallurgy,  
Belgrade, Serbia, <sup>2</sup>Retired from the University of Belgrade, Institute for  
Multidisciplinary Research, Belgrade, Serbia

Scientific paper

ISSN 0351-9465, E-ISSN 2466-2585

<https://doi.org/10.62638/ZasMat1039>



Zastita Materijala 65 (1)

3 - 10 (2024)

## Correct determination of the hydrogen evolution reaction parameters at Ni foam electrode modified by electrodeposited Ni-Sn alloy layer

### ABSTRACT

The example of the procedure for the correct determination of the parameters of hydrogen evolution reaction (HER), the exchange current density ( $j_0$ ) and relaxation time ( $\tau_0$ ) for intermediate (adsorbed hydrogen,  $H_{ads}$ ) adsorption at modified porous Ni-based electrode are presented in this work. Such a procedure is applicable for the HER at all electrode materials. The value of  $j_0$  was obtained from the intercept at  $\eta = 0$  mV from the  $\eta$  vs.  $\log(R_{ct}^{-1})$  dependence ( $\eta$  - overpotential), while the value of  $\tau_0$  was obtained from the intercept at  $\eta = 0$  mV from the  $\log \tau$  vs.  $\eta$  dependence. It was shown that for the correct determination of  $j_0$  and  $\tau_0$ , it is necessary to correct applied  $\eta$  for the  $jR_s$  drop, by recording current density ( $j$ ) for applied  $\eta$  and correcting it for  $jR_s$ .

**Keywords:** HER parameters, exchange current density, relaxation time, Ni-Sn alloy, Ni foam, 30% KOH

### 1. INTRODUCTION

As one of the most investigated electrochemical reactions, the HER was the subject of many chapters and books by different authors, with some of them being cited here [1-6]. The mechanism and kinetics of the HER were mainly studied by Tafel plots analysis and electrochemical impedance spectroscopy (EIS) investigations. Since it was shown that by Tafel plots analysis it is not possible to determine the influence of overpotential on the electrosorption/electrodesorption of active intermediate [7] and that only EIS measurements can provide sufficient data for this process, in this introduction (as well as in the paper) only EIS results for the HER were considered [8-21].

The first theoretical treatment of the electro-sorption / electrodesorption of active intermediate was presented in the work of R.D. Armstrong et al. [8], where the impedance of electrochemical reaction with an adsorbed intermediate without diffusion has been analyzed. At that time a constant phase element (CPE) had not yet been introduced in the literature and the equivalent circuit for intermediate

adsorption (shown in Figure 1) was composed of the charge transfer resistance ( $R_{ct}$ ) of the HER in series with the adsorption pseudocapacitance ( $C_p$ ), and the charge transfer resistance of the electrodesorption of intermediate ( $R_p$ ) connected in parallel. It was assumed that the rate of the formation of the intermediate is  $v_1$ , while the rate of its disappearance is  $v_2$ . In the steady-state  $v_1 = v_2$  and the concentration of intermediate at the surface is given by equation

$$\frac{d\Gamma}{dt} = v_1 - v_2 \quad (1)$$

while relaxation time ( $\tau$ ) is defined as

$$\tau = \left[ \left( \frac{\partial v_2}{\partial \Gamma} \right)_E - \left( \frac{\partial v_1}{\partial \Gamma} \right)_E \right]^{-1} \quad (2)$$

and

$R_0$  (additional resistance at zero frequency) as

$$\frac{1}{R_0} = \tau \left[ n_1 F \left( \frac{\partial v_1}{\partial \Gamma} \right)_E + n_2 F \left( \frac{\partial v_2}{\partial \Gamma} \right)_E \right]^{-1} \left[ \left( \frac{\partial v_1}{\partial E} \right)_E - \left( \frac{\partial v_2}{\partial E} \right)_E \right] \quad (3)$$

Where

$n_1$  is the number of electrons involved in the formation of one molecule of intermediate and  $n_2$  is the number of electrons involved in its disappearance.

\*Corresponding author: Vladimir D. Jović

E-mail: vladajovic@imsi.bg.ac.rs

Paper received: 12. 11. 2023.

Paper accepted: 01. 12. 2023.

Paper is available on the website: [www.idk.org.rs/journal](http://www.idk.org.rs/journal)

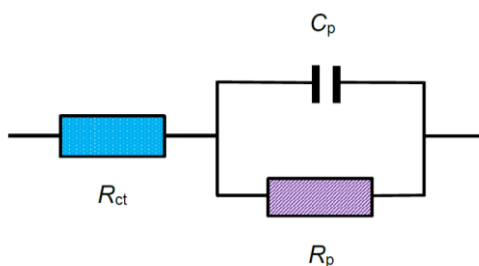


Figure 1. Equivalent circuit for the electroadsorption / electrodeadsorption of active intermediate [8]

Slika 1. Ekvivalentno kolo za reakciju elektrosorpcije / elektrodesorpcije intermedijara [8]

By the analysis of the impedance of this equivalent circuit following equations were derived:

$$R_p = -\frac{R_{ct}^2}{R_0 + R_{ct}} \quad (4)$$

$$C_p = -\frac{R_0 \tau}{R_{ct}^2} \quad (5)$$

Detailed analysis of the obtained impedance equations predicted three general shapes of Nyquist plots [8]:

- (1)  $R_0 \gg R_{ct}$  – the equivalent circuit is reduced to the parallel connection of  $R_{ct}$  and  $C_{dl}$  producing one semi-circle;
- (2)  $R_0$  comparable to  $R_{ct}$  – if  $R_{ct}C_{dl} \ll \tau$  two semi-circles will appear on the Nyquist plot, one at high frequencies ( $\omega \geq 1/R_{ct}C_{dl}$ ) corresponding to the parallel connection of  $R_{ct}$  and  $C_{dl}$  and another one at low frequencies ( $\omega \leq 1/\tau$ ) corresponding to the parallel connection of  $R_p$  and  $C_p$ ;
- (3)  $R_0 \ll R_{ct}$  – producing complex shapes of Nyquist plots depending on the values of parameters.

In 1982 Harrington et al. [16] provided a detailed theoretical analysis for such a case considering the same equivalent circuit as that in Ref. [8] connected in parallel with the double layer capacitance ( $C_{dl}$ ) by discussing the significance of the equivalent circuit elements on the behavior of a multi-step reaction with the adsorbed intermediate in the absence of diffusion control. The best example for this analysis was the HER. The total impedance was given by the equation

$$Z = \frac{1}{\left[ R_{ct} + \frac{1}{\left( \frac{1}{R_p} + j\omega C_p \right)} \right]^{-1} + j\omega C_{dl}} \quad (6)$$

Where

$R_{ct}$  is the charge transfer resistance of the HER,  $R_p$  is the charge transfer resistance of the electrodeadsorption step and/or recombination step, and  $C_p$  is the pseudo-capacitance of the electroadsorbed species. The capacitance  $C_p$  was assumed to appear in combination with the resistor  $R_p$ .

There are in the literature only a few papers presenting experimentally obtained results for the parameters  $R_p$  and  $C_p$  [17-21]. In Ref. [17] the HER at a rotating Pt electrode was investigated in 0.5 M NaOH and 0.5 M  $H_2SO_4$  by EIS measurements. Nyquist plots in both solutions were characterized by two semi-circles with the values of  $C_p$  being one order of magnitude higher than the values of  $C_{dl}$ , increasing with the overpotential, while  $R_p$  values decreased with the overpotential increase. Two semi-circles were also obtained for the EIS of HER on modified (Ni-Al-Cu-Cr) and pure Rensay nickel electrode (Ni-Al) in 5.36 M KOH at 70 °C, with  $C_p$  increasing and  $R_p$  decreasing with the overpotential [18]. Kinetics and mechanism of the HER at electrodeposited Ni/NiMoS<sub>2</sub> electrode in 6 M KOH at 25 °C were also investigated by EIS measurements in the work of Castro et al. [19]. Again, two semi-circles in Nyquist plots were obtained, but the values of  $C_p$  and  $R_p$  as a function of overpotential were not presented. The same equivalent circuit (as that in Refs. [16] and [17]) was used to fit EIS results of the HER at Pd-Ni alloys in 0.5 M NaOH at 25 °C. Fitting results showed that the values of  $C_p$  and  $C_{dl}$  are comparable as a consequence of hydrogen absorption at the electrode surface reducing available electrode surface for the HER to only 10 % [20]. In Ref. [21] the HER was investigated in 0.1 M  $H_2SO_4$  at a rough Pd rotating electrode. EIS results were fitted with the equivalent circuit presented in Figure 5, since all Nyquist plots were characterized with well-defined two semi-circles. It was shown that the value of  $C_p$  is practically independent of overpotential, with the value of  $d\eta/d\log R_p$  being  $\sim 0.062$  V dec<sup>-1</sup>. Such behavior was explained by the fact that hydrogen adsorption does not follow Langmuir adsorption isotherm.

The procedure of interpretation of the experimental results and calculation of correct values of parameters for the HER at Ni-Sn coated Ni foam by the analysis of EIS results is presented in this work.

## 2. EXPERIMENTAL

### 2.1. Sample preparation

All solutions were made from p.a. chemicals (Sigma-Aldrich) in extra pure (18.2 MΩ) UV water (Smart2, Pure UV, TKA). Ni foam with average open pore size of 800 μm was used as a substrate

for electrodeposition. In order to remove oxide from the Ni surface Ni foam substrate was first soaked in acetone for 10 min. with ultrasonication. The next step was cleaning in 1.0 M HCl solution in an ultrasound bath for 10 min., while the final step was ultrasonication for 5 min. in deionized water. Pretreatment of Ni foam was performed at room temperature. Such sample was used for the electrodeposition of Ni-Sn alloy on it. The sample was made by the procedure shown in Figure 2 [22]. The foam was cut into dimensions 2 cm x 1 cm. Half of the foam (1 cm) was covered with the L-shaped Ni mesh 40 (2.5 cm x 1 cm) and pressed to provide good contact between the foam and Ni mesh 40. This part of the electrode, as well as part of Ni mesh, were isolated with Teflon tape (foil) in order to prevent contact with the electrolyte. The top of the Ni mesh was soldered for Ni wire and placed in a glass tube in such a way that electrolyte could not enter the tube.

The geometric surface area ( $S_g$ ), as well as the real surface area (RSA), are presented in Table 1. The RSA was obtained by BET analysis (Brunauer–Emmett–Teller), where BET surface areas were measured by krypton adsorption at 77.3 K according to DIN ISO 9277 (Autosorb AS-1). The values given in Table 1 were obtained for

pure Ni foam without Ni-Sn coating on the Ni foam [22].

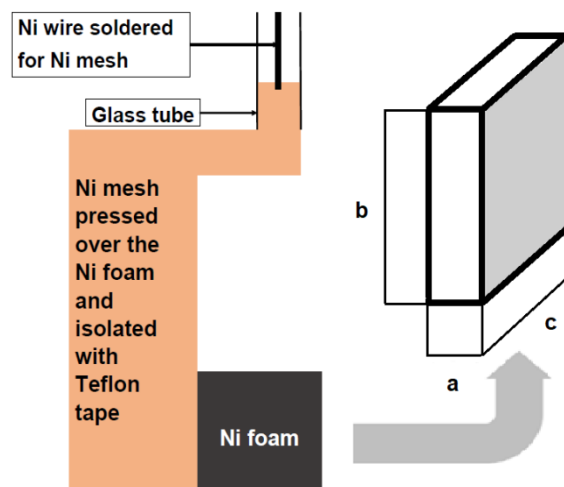


Figure 2. Schematic presentation of the Ni foam working electrode. Geometric electrode surface area was calculated by the equation:

$$S_g = 2ab + (a + 2b) \cdot c \quad [22]$$

Slika 2. Shematski prikaz elektrode od Ni pene. Geometrijska površina elektrode je izračunata pomoću jednačine:  $S_g = 2ab + (a + 2b) \cdot c$  [22]

Table 1. Geometric surface area ( $S_g$ ) and the value of RSA for Ni foam

Tabela 1. Geometrijska površina elektrode ( $S_g$ ) i vrednost realne površine elektrode (RSA) za Ni penu

Ni foam	Specification (cm <sup>2</sup> /cm <sup>3</sup> )	$S_g$ (cm <sup>2</sup> )	V (cm <sup>3</sup> )	RSA (cm <sup>2</sup> )	RSA / $S_g$
800 μm	83	3.16	0.282	23.406	7.41

The H-type electrochemical cell was used for the HER testing.

The Ni foams are commercially available as a mass product for different applications. Ni foam (Alantum) was used as a substrate for the electrodeposition of Ni-Sn alloy coating.

### 2.2. Electrodeposition of Ni-Sn alloy on Ni foam substrate

The electrodeposition of Ni-Sn coating on Ni foam substrate was performed by means of a potentiostat Interface 1010E (Gamry Instruments Inc.) at constant current density of  $j_{dep} = -40$  mA cm<sup>-2</sup> for 2000 s in the bath containing 0.6 M K<sub>4</sub>P<sub>2</sub>O<sub>7</sub> + 0.1 M NiCl<sub>2</sub>·6H<sub>2</sub>O + 0.03 M SnCl<sub>2</sub>·2H<sub>2</sub>O + 0.3 M NH<sub>2</sub>CH<sub>2</sub>COOH (pH 6.7) at the room temperature.

### 2.3. HER polarization curves

The HER polarization characteristic at the investigated electrode was tested in 30 % KOH solution at the temperature of 70 °C. The sample was first submitted to HER at a constant current

density  $j = -300$  mA cm<sup>-2</sup> for 600 s ( $j$  was calculated using geometric surface area  $S_g$  – see Table 1). The polarization curves were recorded using linear sweep voltammetry (LSV) at the sweep rate of 1 mV s<sup>-1</sup> by two procedures: (1) Without  $iR_s$  drop correction, starting from  $\eta = -50$  mV and finishing at  $\eta = -110$  mV; (2) Using current interrupt technique, starting from  $\eta = -20$  mV up to the  $\eta$  at which the current reached maximum value of 1 A (limit of the potentiostat).

### 2.4. HER investigation by EIS

EIS measurements were performed in the same cell with the same potentiostat, using software EIS 300 (Gamry Instruments Inc.): amplitude 5 mV RMS, 20 points per decade, starting at 20 kHz and finishing at 0.01 Hz at four values of  $\eta$ : -50 mV, -70 mV, -90 mV and -110 mV. Before recording EIS results, sample was held at the potential of the EIS measurements for 100 s to establish a stable current density response. Fitting of the experimental results was carried out by

Echem Analyst software – EIS 300 (Gamry Instruments Inc.).

### 3. RESULTS AND DISCUSSION

#### 3.1. Polarization curves for the HER

The polarization curve measured without  $jR_s$  correction and polarization curve corrected for  $jR_s$  for the HER at Ni-Sn/Ni foam 800 sample in 30 % KOH at 70 °C are shown in Figure 3.

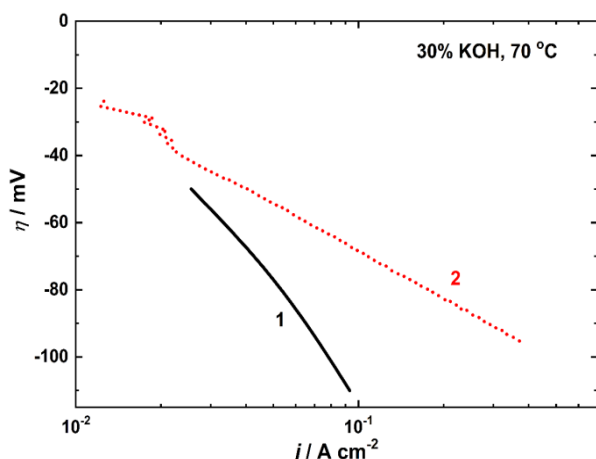
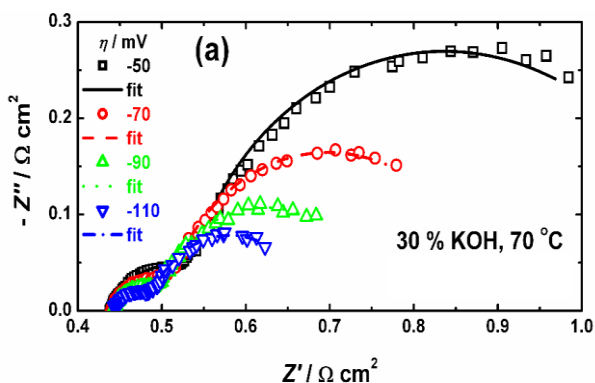


Figure 3. Polarization curves for the HER at investigated sample in 30 % KOH at 70 °C: (1) Without  $jR_s$  drop correction; (2) With  $jR_s$  drop correction using current interrupt technique

Slika 3. Polarizacione krive za izdvajanje vodonika na ispitivanoj elektrodi u 30 % KOH na temperaturi od 70 °C: (1) Bez korekcije za pad napona  $jR_s$ ; (2) Sa korekcijom za pad napona  $jR_s$

Curve 1 corresponds to the measurement without  $jR_s$  correction, while curve 2 represents the measurement with current interrupt  $jR_s$  correction. As can be seen, the same overpotential has been



reached at a higher current density for the  $jR_s$  drop corrected curve.

#### 3.2. HER investigation by EIS

Nyquist plots recorded at four overpotentials (-50 mV, -70 mV, -90 mV and -110 mV) are presented in Figure 4. All Nyquist plots are characterized by the presence of two semi-circles, one at high frequencies corresponding to the charge transfer and the other one at low frequencies, which could only be ascribed to the overpotential-dependence of the process of electroadsorption / electrodeadsorption of  $H_{ads}$  intermediate. Those Nyquist plots were fitted with the equivalent circuit shown in Figure 5. The values of  $C_p$  were calculated using the equation [23,24]

$$C_p = \left[ Y_p R_p^{(\alpha_p - 1)} \right]^{\frac{1}{\alpha_p}} \quad (7)$$

with  $Y_p$  being the constant of  $CPE_p$  and  $\alpha_p$  being the exponent. Obtained values for  $R_{ct}$ ,  $C_p$  and  $R_p$  were used for further calculation.

According to Armstrong et al. [8] marked part of the equivalent circuit presented in Figure 5 corresponds to the process of intermediate electroadsorption / electrodeadsorption. Using obtained values for  $R_{ct}$ ,  $C_p$  and  $R_p$ , the values of  $R_o$  and  $\tau$  were calculated by the following equations:

$$R_o = \frac{-R_{ct}(1+R_p)}{R_p} \quad (8)$$

$$\tau = \frac{-C_p(R_{ct}^2)}{R_o} \quad (9)$$

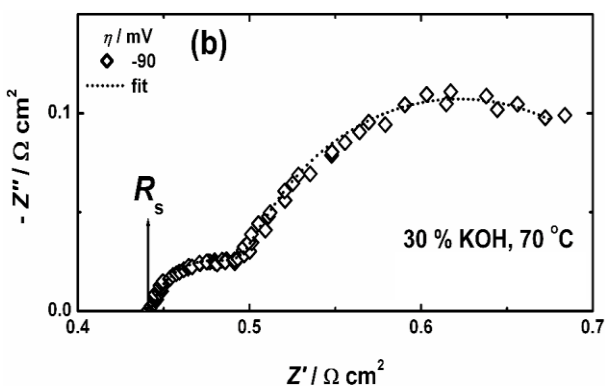


Figure 4. Nyquist plots recorded at different overpotentials in 30 % KOH at 70 °C. Squares, circles and triangles represent experimental points, while lines (solid, dotted, dashed and dash-dot) correspond to the fitting curves

Slika 4. Nyquist-ovi dijagrami registrovani pri različitim vrednostima prenapetosti u 30 % KOH na temperaturi od 70 °C. Kvadrati, krugovi i trouglovi predstavljaju eksperimentalne tačke, a linije (puna, tačkasta, isprekidana i tačka-crtica) odgovaraju krivama fitovanja

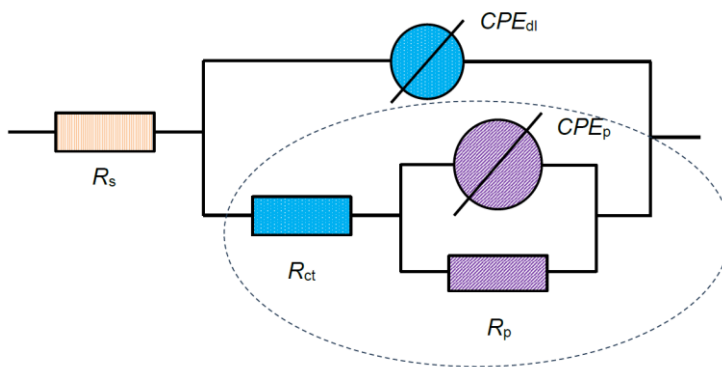


Figure 5. Equivalent circuit for fitting Nyquist plots presented in Figure 4:  $R_s$  – solution resistance;  $R_{ct}$  – charge transfer resistance;  $CPE_{dl}$  – constant phase element corresponding to double layer capacitance;  $CPE_p$  - constant phase element corresponding to adsorption pseudo capacitance and  $R_p$  - charge transfer resistance of the electrosorption / electrodesorption of intermediate

Slika 5. Ekvivalentno kolo za fitovanje Nyquist-ovih dijagrama prikazanih na slici 4:  $R_s$  – omski otpor elektrolita;  $R_{ct}$  – otpor razmene naelektrisanja;  $CPE_{dl}$  – konstantni fazni element koji odgovara kapacitetu dvojnog sloja;  $CPE_p$  - konstantni fazni element koji odgovara kapacitetu adsorpcije intermedijara;  $R_p$  - otpor razmene naelektrisanja pri electrosorpciji / electrodesorpciji intermedijara

As stated in the Section 2.4. before recording EIS results, sample was held at applied overpotential for 100 s to establish a stable current density response. Since the EIS measurements cannot be performed with  $jR_s$  drop compensation, the current density for each overpotential was recorded for 100 s, as shown in Figure 6. As can be seen after the initial decrease of the current density well-defined plateaus were established.

In order to obtain the values of  $\eta$  corrected for  $jR_s$  drop, the values of current density plateaus ( $j$ ) were multiplied with the values of solution

resistance ( $R_s$ ) and subtracted from the applied overpotentials by the equation:

$$|\eta_{corr.}| = |\eta| - |jR_s| \tag{11}$$

In Table 2 are given the absolute values of  $j$  and  $R_s$ , as well as uncorrected and corrected overpotentials ( $\eta$  and  $\eta_{corr.}$ ). Hence, it is obvious that the applied overpotential is higher than the corrected one, and this (corrected) value should be used for determining the real values of  $j_0$  and  $\tau_0$ .

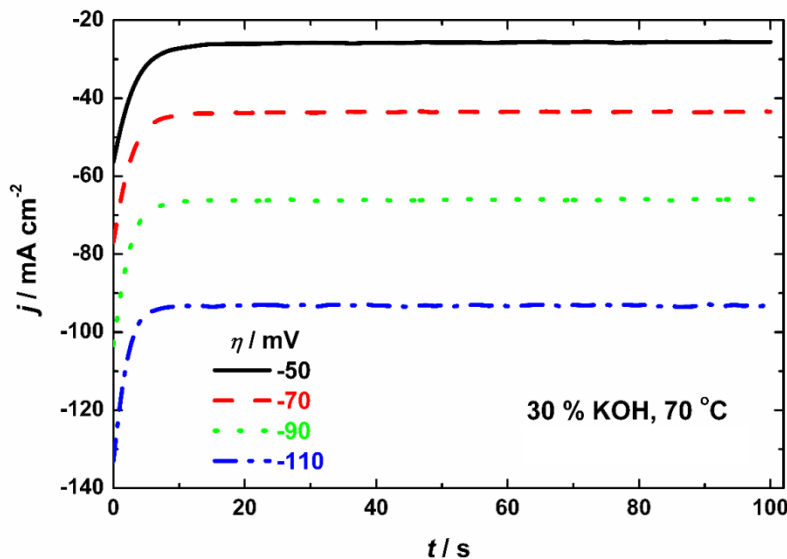


Figure 6.  $j$  vs.  $t$  responses for different values of  $\eta$  before the EIS measurements at these overpotentials

Slika 6.  $j$  - $t$  odgovori pri različitim vrednostima prenapetosti pre impedansnih merenja na tim prenapetostima

Table 2. Applied ( $\eta$ ) and corrected ( $\eta_{\text{corr}}$ ) values of the overpotentialsTabela 2. Zadate ( $\eta$ ) i korigovane ( $\eta_{\text{corr}}$ ) vrednosti prenapetosti

$ \eta / \text{V} $	$R_s / \Omega \text{ cm}^2$	$ j / \text{A cm}^{-2} $	$ j R_s / \text{V} $	$ \eta_{\text{corr}} / \text{V} $
0.05	0.43891	0.02559	0.01123	0.03959
0.07	0.43942	0.04346	0.0191	0.05233
0.09	0.44247	0.06591	0.06285	0.06285
0.11	0.44399	0.09303	0.0413	0.07163

In Figure 7(a) are presented  $\eta$  vs.  $\log(R_{\text{ct}}^{-1})$  and  $\eta_{\text{corr}}$  vs.  $\log(R_{\text{ct}}^{-1})$  dependences. It is obvious that the value of  $j_0(\text{corr.})$  obtained from  $\eta_{\text{corr}}$  vs.  $\log(R_{\text{ct}}^{-1})$  dependence is much lower, and that particular value should be used for the correct determination of  $j_0$ . In Figure 7(b) are presented  $\log \tau$  vs.  $\eta_m$  and  $\log \tau$  vs.  $\eta_{\text{corr}}$  dependencies with  $\tau_0$  and  $\tau_0(\text{corr.})$  corresponding to measured and

correct values of  $\tau$ , respectively. The values of  $j_0$  and  $j_0(\text{corr.})$  were calculated using equation

$$j_0 = \frac{RT}{zF} \frac{1}{R_{\text{ct}}^0} \quad (11)$$

with  $1/R_{\text{ct}}^0$  representing the intercept at the x axis for  $\eta = 0$  (Figure 7(a)).

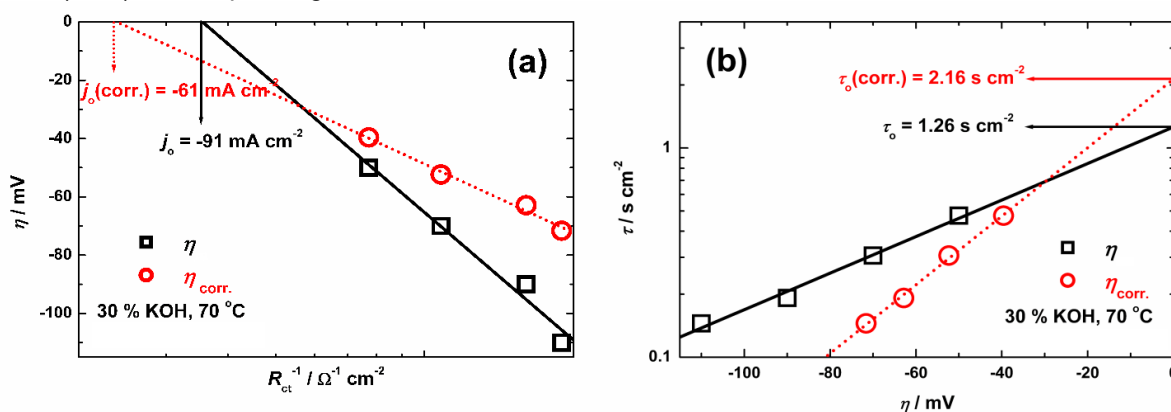


Figure 7. (a)  $\eta_m$  vs.  $\log(R_{\text{ct}}^{-1})$  and  $\eta_{\text{corr}}$  vs.  $\log(R_{\text{ct}}^{-1})$  dependences for the HER at investigated electrode in 30 % KOH at 70 °C. (b)  $\log \tau$  vs.  $\eta_m$  and  $\log \tau$  vs.  $\eta_{\text{corr}}$

Slika 7. (a)  $\eta_m$  vs.  $\log(R_{\text{ct}}^{-1})$  and  $\eta_{\text{corr}}$  vs.  $\log(R_{\text{ct}}^{-1})$  za izdvajanje vodonika na ispitivanoj elektrodi u 30 % KOH na temperaturi od 70 °C. (b)  $\log \tau$  vs.  $\eta_m$  and  $\log \tau$  vs.  $\eta_{\text{corr}}$

All obtained values correspond to the geometric surface area  $S_g$ . Assuming that the RSA for pure Ni foam and that covered with the Ni-Sn coating is the same, the values given in Figure 7 should be divided by 7.41 (see Table 1) in order to obtain values of  $j_0$  and  $\tau_0$  expressed per real surface area.

#### 4. CONCLUSIONS

In order to obtain correct values of the parameters of HER at any type of electrode materials, the exchange current density ( $j_0$ ) and relaxation time ( $\tau$ ) for intermediate ( $\text{H}_{\text{ads}}$ ) adsorption, the procedure explained in this work should be used. The value of  $j_0$  was obtained from the intercept at  $\eta = 0$  mV from the  $\eta$  vs.  $\log(R_{\text{ct}}^{-1})$  dependence, and the value of  $\tau_0$  was obtained from the intercept at  $\eta = 0$  mV from the  $\log \tau$  vs.  $\eta$

dependence. It was shown that for the correct determination of  $j_0$  and  $\tau_0$ , it is necessary to correct applied  $\eta$  for the  $jR_s$  drop, by recording current density ( $j$ ) for applied  $\eta$  and correcting it for  $jR_s$ .

#### Acknowledgements

This work was supported by the Federal Ministry of Education and Research – Germany, through the WBC2019 call – project NOVATRODES 01DS21010 and by the Ministry of Science, Technological Development and Innovation of the Republic of Serbia, contract no. 451-03-47/2023-01/200135.

SPONSORED BY THE



## 5. REFERENCES

- [1] S.Trasatti (1992) Electrolysis of Hydrogen Evolution: Progress in Cathode Activation, In: H. Gerischer, C.W. Tobias (Eds.), *Advances in Electrochemical Science and Engineering*, Wiley-VCH, Weinheim, p. 2–85.
- [2] B.V.Tilak, P.W.T.Lu, J.E.Colman, S.Srinivasan (1981) Electrolytic Production of Hydrogen, In: *Comprehensive Treatise of Electrochemistry*, J.O'M. Bockris, B.E. Conway, E. Yeager, R.E. White (Eds.), Vol. 2, Plenum Press, New York and London, p. 1-97.
- [3] V.D.Jović, N.V.Krstajić, T.Rauscher (2023) Electrodeposited Ni-Based, Non-Noble Metal Cathodes for a Hydrogen Evolution Reaction in Alkaline Solutions, In: M.J. Acosta (Ed.), *Advances in Energy Research*, Vol. 39, Nova Science Publishers, Inc., New York, p. 97-184.
- [4] A.Lasia (2003) Hydrogen evolution reaction, In: W. Vielstich, A. Lamm, H.A. Gasteiger (Eds.), *Handbook of Fuel Cells – Fundamentals, Technology and Applications*, Vol. 2, John Wiley & Sons, Ltd., Chichester, p 416-440.
- [5] Noble-Metal-Free Electrocatalysts for Hydrogen Energy, *Catalytic Science Series*, Vol. 20, Q. Gao, L. Yang (Eds.), World Scientists, 2022.
- [6] B.E.Conway, B.V.Tilak, in: D.D. Eley, H.Pines, P.B. Weisz (Eds.) (1992) *Advances in Catalysis*, vol. 38, Academic Press, Inc., San Diego, California, Ch. 1.
- [7] H.Gerischer, W.Mehl, Z.Elektrochem (1955) Zum Mechanismus der kathodischen Wasserstoffabscheidung an Quecksilber, Silber und Kupfer, *Z. Physic. Chem*, 59, 1049-1059.
- [8] R.D.Armstrong, M.Henderson (1972) Impedance plane display of a reaction with an adsorbed intermediate, *J. Electroanal. Chem.*, 39, 81-90.
- [9] S.-I. Pyun, T.-H.Yang (1996) Investigation of the HER at a 10 wt. Pd-dispersed C electrode using EIS, *J. Appl. Electrochem.*, 26, 953-958.
- [10] C.Hitz, A.Lasia (2001) Experimental study and modeling of impedance of the her on porous Ni electrodes, *J. Electroanal. Chem.*, 50, 213-222.
- [11] A.Lasia (2002) Applications of electrochemical impedance spectroscopy to hydrogen adsorption, evolution and absorption into metals, in: B.E. Conway, R.E. White (Eds.), *Modern Aspects of Electrochemistry*, no. 35, Kluwer Academic Publishers, New York, Boston, Dordrecht, London, Moscow, Ch. 1.
- [12] B.Losiewicz, A.Budniok, E.Rowinski, E.Lagiewka, A. Lasia (2004) The structure, morphology and electrochemical impedance study of the hydrogen evolution reaction on the modified nickel electrodes, *Int. J. Hydrogen Energy*, 29, 145-157.
- [13] L.Birry, A.Lasia (2004) Studies of the hydrogen evolution reaction on Raney nickel–molybdenum electrodes, *J. Appl. Electrochem.*, 34, 735–749.
- [14] B.E.Castro, R.H.Milocco (2005) Identifiability of sorption and diffusion processes using EIS: Application to the hydrogen reaction, *J. Electroanal. Chem.*, 579, 113-123.
- [15] A.Lasia (2019) Mechanism and kinetics of the hydrogen evolution reaction, *Int.J.Hydrogen Energy*, 44, 19484-19518.
- [16] D.A.Harrington, B.E.Conway (1987) Ac impedance of faradaic reactions involving electroadsorbed intermediates - I. Kinetic theory, *Electrochim. Acta*, 32, 1703-1712.
- [17] L.Bai, D.A.Harrington, B.E.Conway (1987) Behavior of overpotential-deposited species in faradaic reactions - II. ac impedance measurements on H<sub>2</sub> evolution kinetics at activated and unactivated Pt cathodes, *Electrochim. Acta*, 32, 1713-1731.
- [18] M.Okido, J.K.Depo, G.A.Capuano (1993) The Mechanism of Hydrogen Evolution Reaction on a Modified Raney Nickel Composite-Coated Electrode by AC Impedance, *J. Electrochem. Soc.*, 40, 127-133.
- [19] E.B.Castro, M.J. de Giz, E.R.Gonzalez, J.R.Vilche (1997) An electrochemical impedance study on the kinetics and mechanism of the hydrogen evolution reaction on nickel molybdenite electrodes, *Electrochim. Acta*, 42, 951-959.
- [20] N.V.Krstajić, S.Burojević, Lj.M.Vračar (2000) The determination of kinetics parameters of the hydrogen evolution on Pd-Ni alloys by ac impedance, *Int.J.Hydrogen Energy*, 25, 635-641.
- [21] D.Lin, A.Lasia (2017) Electrochemical impedance study of the kinetics of hydrogen evolution at a rough palladium electrode in acidic solution, *J. Electroanal. Chem.*, 785, 190-195.
- [22] J.D.Gojgić, A.M.Petričević, T.Rauscher, C.I. Bernäcker, T.Weißgärber, L.Pavko, R.Vasilić, M.N. Krstajić Pajić, V.D.Jović (2023) Hydrogen evolution at Ni foam electrodes and Ni-Sn coated Ni foam electrodes, *Applied Catalysis A, General*, 663, 119312
- [23] C.H.Hsu, F.Mansfeld (2001) Technical Note: Concerning the Conversion of the Constant Phase Element Parameter  $Y_0$  into a Capacitance, *Corr.* 57, 747-748.
- [24] V.D. Jović (2022) Calculation of a pure double layer capacitance from a constant phase element in the impedance measurements, *Zaštita Materijala*, 63, 50-57.

## IZVOD

### PROCEDURA KOREKTNOG ODREĐIVANJA PARAMETARA REAKCIJE IZDVAJANJA VODONIKA NA ELEKTRODI OD NI PENE MODIFIKOVANE ELEKTROHEMIJSKI ISTALOŽENOM Ni-Sn LEGUROM

Na primeru izdvajanja vodonika na Ni-Sn/Ni pena 800 elektrodi u ovom radu je prikazana procedura korektnog određivanja parametara ove reakcije, a to su: gustina struje izmene ( $j_0$ ) i relaksaciono vreme adsorpcije intermedijara ( $\tau$ ) ( $H_{ads}$ ). Vrednost  $j_0$  je određena iz odsečka za  $\eta = 0$  mV zavisnosti  $\eta$  vs.  $\log(R_{ct}^{-1})$  ( $\eta$  - prenapetost), dok je vrednost  $\tau_0$  određena iz odsečka za  $\eta = 0$  mV zavisnosti  $\log \tau$  vs.  $\eta$ . Pokazano je da je za korektno određivanje ovih parametara neophodno korigovati gustinu struje pri svakoj zadatoj prenapetosti za vrednost omskog pada napona  $jR_s$ .

**Ključne reči:** Reakcija izdvajanja vodonika, gustina struje izmene, relaksaciono vreme, Ni-Sn legura, Ni pena, 30 % KOH

Naučni rad

Rad primljen: 12.11.2023.

Rad prihvaćen: 01.12.2023.

Rad je dostupan na sajtu: [www.idk.org.rs/casopis](http://www.idk.org.rs/casopis)